## T.2: Free Electron Lasers

**K.K. Pant**
*Free Electron Laser Laboratory*
*Materials & Advanced Accelerator Sciences Division*
*E-mail: kkpant@rrcat.gov.in*

**Abstract:**

A free electron laser (FEL) is an electron beam based tunable source of coherent electromagnetic (EM) radiation. The operating principle of an FEL involves a resonant exchange of energy between a beam of electrons and a co-propagating electromagnetic wave inside a spatially periodic arrangement of magnets, called an undulator. FELs have the same principle of operation over the complete electromagnetic spectrum, and the pulse structure of the EM radiation generated by an FEL mimics the pulse structure of its electron beam. Worldwide, FELs have been built at wavelengths ranging from millimeter waves to hard X-rays, with different peak powers and pulse structure - from femtosecond (fs) pulses with Gigawatt (GW) power at hard X-ray wavelength to picosecond (ps) pulses of Megawatt (MW) power at millimeter (mm) wave length. RRCAT has an on-going long-term, three-stage FEL program under which an Infra-red Free Electron Laser (IR-FEL) is presently in an advanced stage of commissioning. This article discusses the principle of operation, important sub-systems, and special features of FELs. A review of the present status of activity at RRCAT and abroad is also discussed.

### 1. Introduction:

A Free electron laser (FEL) is a tunable source of high power coherent radiation in which a fraction of the energy carried by a relativistic electron beam is transferred resonantly to a co-propagating electromagnetic wave in the presence of a spatially periodic arrangement of magnets, called an undulator. The first successful operation of an FEL was demonstrated by Madey et al in 1976, and since then FELs have been built at wavelengths from millimeter (mm) waves to hard X-rays. A very simple and illuminating description of the science and technology of FELs is given in Reference [1].

The wavelength $\lambda_L$ of radiation generated in a FEL depends upon the wavelength, or period, of the undulator magnetic field $\lambda_U$, the relativistic gamma factor ($\gamma$) of the electrons, and the undulator parameter $K_U = eB_U\lambda_U/2\pi mc$, and is given by the expression

$$\lambda_L = \frac{\lambda_U}{2\gamma^2}(1 + K_U^2) \qquad (1)$$

Here, e and m are the electronic charge and mass respectively, $B_u$ is the peak undulator magnetic field, and $c$ is the velocity of light in free space. Wavelength of an FEL can be tuned mainly by varying the $\gamma$ of the electron beam. To a smaller extent, it can also be tuned by varying the undulator parameter $K_u$. Tunability of wavelength of an FEL from 0.23 μm to 100 μm using five undulators has been demonstrated at the Free Electron Laser Institute (FELI) in Japan.

Since the pulse structure of EM radiation from an FEL mimics the pulse structure of the electron beam, FELs using S-band linacs have been operated mostly with a pulse width of a few picosecond, which is the typical electron beam pulse width from an S-band linac structure. With the recent progress in bunch compression technology, X-ray FELs based on S-band linacs have also demonstrated operation with femtosecond (fs) pulses, which gives users a cutting edge tool to probe a variety of ultra-fast phenomenon taking place in nature. In the visible/Infra-red (IR)/Ultraviolet (UV) regions, FELs are not as competitive as conventional lasers since they require large sub-systems like accelerators, electron beam transport line and undulators. They are mainly built at wavelengths ranging from far infra-red to mm waves, a spectral region where other radiation sources like conventional lasers or microwave sources are either not very efficient, or are not available at all. At the other end of the spectrum, X-ray FELs represent the state-of-the-art in the field, and these FELs are coupled to state-of-the-art accelerator facilities.

### 1. Principle of operation:

Figure T.2.1 shows a schematic of an FEL where a beam of relativistic electrons from an accelerator is propagated along the axis of an undulator, which supports a spatially periodic magnetic field given by Eq. (2), where $k_U = 2\pi/\lambda_U$.

$$\boldsymbol{B}_U = B_U \sin(k_U z)\boldsymbol{y}. \qquad (2)$$

The field strength of an undulator is given by the undulator parameter $K_U = eB_U\lambda_U/2\pi mc$. For FELs, $K_U \sim 1$ or slightly less than 1 and the magnetic arrangement is called as an undulator. For $K_U >> 1$, as in Synchrotron Radiation Sources (SRS), the device is called as a wiggler.

An electron initially moving with a velocity $v_{0z}$ along 'z' direction experiences a Lorentz force in the 'x' direction due to the undulator magnetic field along the 'y' direction. Since the magnetic field is spatially periodic along the 'z' direction, the Lorentz force has the same periodicity. Consequently, the electron executes a snake-like wiggly motion in the x-z plane

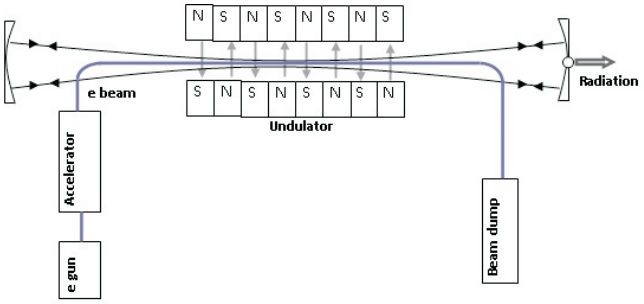


*Fig. T.2.1: Schematic of an FEL with its important sub-systems.*

as it propagates along the undulator, with the 'x' component of its velocity given by

$$\boldsymbol{v_x} = v_x \sin(k_U z)\boldsymbol{x}. \quad (3)$$

A relativistic electron initially moving with a constant velocity along the 'z' direction now becomes an accelerated charged particle due to the wiggly motion, and emits radiation as dictated by the laws of electrodynamics, with the wavelength of radiation given by Eq. (1). Each electron bunch from an RF linac has a large number of electrons which are assumed to be distributed uniformly along the length of each bunch. Since all electrons radiate randomly as they propagate through the undulator, the net radiation coming out of the undulator is 'spontaneous emission' with a pulse length equal to the bunch length of electrons from the RF linac. The principle of superposition dictates that the Power in this spontaneous radiation is proportional to $N_e$, the number of particles in the bunch. This spontaneous emission of radiation is identical to radiation obtained from Synchrotron Radiation Sources.

The amplitude of transverse oscillations executed by an electron inside an undulator is given by $K_u/\gamma$. Further, a relativistic charged particle emits radiation in a direction perpendicular to its oscillation, with a maximum intensity at 90 degrees to the oscillatory motion. This radiation is concentrated in a narrow cone with a semi-angle $1/\gamma$. For $K_u \sim 1$, as is the case of most FELs, the amplitude of transverse oscillations of the electrons and the solid angle of radiation emitted by the oscillating electrons are both $\sim 1/\gamma$. Therefore, an observer at the end of the undulator receives radiation from the full transverse oscillation executed by the electron, and this overlap between transverse oscillations and the radiation cone of semi-angle $1/\gamma$ also helps in the build-up of coherence in an FEL. This is discussed in greater detail later in this article. On the other hand, for a wiggler with $K_u >> 1$ as in the case of a SRS, the transverse excursion of electrons is much greater than the solid angle of radiation emitted by the oscillating charge. Consequently, an observer at the end of the wiggler receives light only for a short duration of the electron motion. Also, the electron does not experience the field of the radiation emitted for a major portion of its trajectory through the undulator, thereby resulting in no or very poor build-up of coherence.

Since an electron radiates only when it propagates through the undulator of length $L_u = N_u\lambda_u$, where $N_u$ is the number of undulator periods, the radiation is emitted only for a finite time and the Fourier transform of this radiation gives the spectral width of undulator radiation, which is equal to $1/2Nu$. Typically, the line width of radiation is of the order of 1% for an FEL with a 50 period undulator.

The build-up of coherence in an FEL results in a brightness of radiation that is greater by orders of magnitude as compared to that from an SRS. In order to understand the build-up of coherence in an FEL, consider that the electron beam propagating through the undulator also sees an electromagnetic wave whose field components are given by

$$\boldsymbol{E}_R = \boldsymbol{x}E_R \cos(k_R z - \omega_R t + \phi_R),$$
$$\boldsymbol{B}_R = \boldsymbol{y}B_R \cos(k_R z - \omega_R t + \phi_R).$$

Here, $E_R$ and $B_R$ are the electric and magnetic fields respectively of the radiation generated at a frequency $f_R = 2\pi/\omega_R$ with a wave vector $k_R = 2\pi/\lambda_R$, $\lambda_R$ being the wavelength of radiation emitted, and $\phi_R$ is an initial phase. These field components could either be due to the incoherent spontaneous radiation emitted by an electron as it enters the undulator, or due to a seed radiation in an amplifier configuration of an FEL. The amplitudes ($E_R$ and $B_R$) and phase $\phi_R$ are slowly varying down the undulator.

The first order Lorentz force experienced by an electron due to the undulator magnetic field imparts to it a transverse velocity $v_x$ given by Eq.(3). As this 'wiggling' electron and the spontaneous radiation emitted by it co-propagate down the undulator, exchange of energy between the electric field $\mathbf{x}E_R$ of the radiation and the $v_x$ motion of the electrons in the undulator is given by

$$mc^2 \frac{d\gamma}{dt} = e\boldsymbol{E_R}.\boldsymbol{v_x}. \quad (5)$$

From Eqs. (3), (4) and (5), one obtains

$$\frac{d\gamma}{dt} \propto -\cos(k_R z - \omega_R t + \phi_R) \sin(k_U z) \quad (6)$$

The right hand side of this equation can be written as $\{\sin(k_R z - k_u z - \omega_R t + \phi_R) - \sin(k_R z + k_u z - \omega_R t + \phi_R)\}$, and when the electron travels through the undulator, the 'sin' terms average out to zero. If the initial electron velocity $v_{z0} = \omega_R / (k_R + k_U)$, the second term does not average out to zero, and a net energy exchange is possible between radiation and the electron in this case.

Consider an electron moving with a constant velocity along the 'z' direction interacting with a co-propagating wave with phase velocity $v_\phi$ and with a component of electric field along the z direction. An electron with a velocity different from the phase velocity of the wave sees randomly fluctuating phases of the electric field, and the net effect of the electric field averages out to zero. However, for an electron with velocity equal to the phase velocity of the co-propagating wave, the phases are synced as the two co-propagate. Consequently, the electron can either gain or lose energy to the wave, or be unaffected depending upon its initial phase.

In an FEL, a similar interaction takes place between the electrons and a ponderomotive wave driven by the second order interaction between the transverse electron velocity $v_x$ due to the undulator and the $B_y$ field of the co-propagating electromagnetic wave. The quantity $\psi = (k_R z + k_u z - \omega_R t)$ is called as the phase of the ponderomotive wave. Depending upon the quantity $\psi + \phi_R$, an electron can either gain or lose energy to the radiation. Electrons are initially uniformly distributed in phase in the electron beam from the accelerator. During propagation of this beam down the undulator with a velocity $v_{z0} = \omega_R / (k_R + k_U)$, electrons in a phase *0* to $\pi$ lose energy, while those lying between $\pi$ to $2\pi$ are accelerated, and there is no net energy exchange. If the electron distribution can somehow be modified with electrons lying only between phases 0 to $\pi$, $2\pi$ to $3\pi$ and so on, all electrons will lose energy to the ponderomotive wave, leading to the growth of radiation.

In an FEL, the re-distribution of electrons takes place as the electron bunches travel down the undulator with a co-propagating electromagnetic wave. The ponderomotive force experienced by the electrons due to the second order interaction of $v_x$ velocity due to the undulator and the $B_y$ field of the radiation has a time and space dependence given by $\sin(k_u z) \cos(k_R z - \omega_R t + \phi_R)$. If the initial electron velocity is chosen appropriately as discussed earlier, a net force acts along the z direction resulting in a re-distribution of electrons in each bunch leading to micro-bunching around the phases 0, $2\pi$, $4\pi$, etc. The separation between bunches is given by $2\pi/(k_U + k_R)$. Since $k_u$ is much much smaller than $k_R$, the bunching is almost at radiation wavelength and radiation emitted by the bunches adds in phase, leading to a coherent output. Figure T.2.2 shows the redistribution of charge leading to micro-bunching. The principle of superposition dictates in this case that the radiated power $P_R$ is proportional to $N_e^2$, which gives orders of higher brightness for the radiation emitted by the FEL as compared to a Synchrotron Radiation Source. An electron bunch with 0.1 nC charge propagating through an undulator contains ~ $10^8$ electrons and spontaneous emission power from this electron bunch is proportional to this number of electrons. Development of micro-bunching at the radiation wavelength in an FEL would ideally result in development of full coherence in the output radiation giving an enhancement of $10^8$ as compared to the spontaneous emission output from the same bunch.

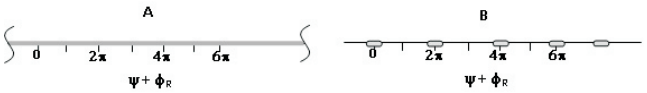


*Fig. T.2.2: Micro-bunching of electrons by the ponderomotive wave. 'A' shows a uniform distribution of electrons over a bunch and 'B' shows electrons micro-bunched around phases 0, π, 2π, etc.*

FELs typically employ S-band radio-frequency (RF) linear accelerators to generate the relativistic electron beam. Electron bunches from a linac operating at 2856 MHz are typically ~ 10ps long, which corresponds to a bunch length ~ 3 mm. For an FEL operating at say 30 μm wavelength, each electron bunch is initially like a uniform distribution, and re-distribution of electrons through micro-bunching has to take place at the wavelength scale of the FEL radiation. As re-distribution of charge in each bunch takes place, coherence is built-up in the output radiation with a consequent increase in power output due to lasing. Although the principle of generation of radiation is the same in a SRS and in a FEL, it is the build-up of coherence in an FEL that results in a power output that is several orders of magnitude higher as compared to the power output from an SRS for the same charge per pulse.

Micro-bunching of charge at the radiation wavelength results in the modulation of an initially uniform distribution of electrons in the electron beam with the same Fourier components ($\omega_R$, $k_R$) as the radiation to be amplified in an

FEL. This drives a current density $J$ with $\omega_R$, $k_R$ Fourier components which, when used in the electromagnetic wave equation given by Eq.(7) yields the growth of radiation.

$$\nabla^2 \boldsymbol{A_R} - \frac{1}{c^2}\frac{d^2 \boldsymbol{A_R}}{dt^2} = -\boldsymbol{J}. \quad (6)$$

Here, $A_R$ ($\omega_R$, $k_R$) is the vector potential associated with the electromagnetic wave, or the FEL radiation. The equation of motion for the electrons in the presence of the undulator magnetic field and the radiation field has to be solved together with Eq. 7 governing the evolution of the radiation field, and the analytical treatment of a FEL involves the solution of these coupled equations as discussed in detail in [1]. Contemporary FELs are all designed using numerical codes that have been developed to solve these coupled equations in three dimensions, considering the time dependence of the evolution of charge distribution and radiation.

## 3. Configurations of operation:

An FEL can be operated in two configurations: as an oscillator or as an amplifier. In an oscillator configuration, the undulator is housed inside an optical cavity and the electron beam from the injector is bent into the optical cavity at the undulatory entry and out of the optical cavity at the undulator exit. The optical pulse reflecting back-and-forth inside the optical cavity interacts with a train of micro-bunches in each electron macro-pulse from the accelerator. Build-up of coherence over several tens of round-trips can be seen from the exponential increase in output power from the FEL in this region, followed by saturation of the FEL interaction. Most operating long wavelength FELs have been built in this configuration. The typical length of the undulator in such FELs is a few meters.

X-ray FELs on the other hand operate in a single-pass amplifier configuration with an undulator length of several tens of meters. The FEL interaction grows as each bunch of electrons with a high peak current travels down the undulator with a co-propagating radiation pulse. Coherence is built-up and the FEL interaction saturates within a single pass resulting in a high peak power output for each electron pulse. Since the amplification process in an X-ray FEL starts from shot noise, this regime of operation is called as Self Amplified Spontaneous Emission (SASE). FELs have also been built at other longer wavelengths in an amplifier configuration. The first successful demonstration of FEL operation by Madey and his team at Stanford University was in an amplifier configuration, which was later repeated by them in an oscillator configuration. Other amplifier configurations with seeding have also been demonstrated at different wavelengths. Currently, there is significant interest in operating short wavelength FELs using harmonic generation schemes, which reduces the requirement of electron beam energy quite significantly. Some examples of such FELs are discussed later in the section reviewing worldwide status of FEL R&D.

## 4. Advantages of FELs

By virtue of its principle of operation, an FEL has certain advantages over conventional lasers and microwave devices with which these are operationally similar. However, they also have certain disadvantages due to the large sizes and expensive nature of different sub-systems required to develop an FEL. Some advantages of an FEL are as follows:

*Tunability:* As can be seen from Eq. (1), the operating wavelength of an FEL can be tuned by changing the energy of the electron beam. It can also be tuned to a lower order by changing the undulator parameter. An example of this tunability is the large wavelength range covered by the FELI FEL in Japan which covers a wavelength range from 0.23 μm to 100 μm using five undulators.

*High power operation:* Since an FEL employs an electron beam propagating through an undulator for the generation of high power radiation, there is no limitation due to material break-down in the interaction region of an FEL. The electron beam is already a broken down medium and the spent beam is extracted from the optical cavity. Therefore, there is no problem of heating inside the optical cavity.

*Choice of pulse structure:* Since FELs have a uniform principle of operation over all wavelengths, it can be designed to generate any desired pulse structure at any wavelength of operation. The pulse structure from an FEL mimics the pulse structure of the electron beam.

## 5. FEL activity at RRCAT

A long-term, three-stage FEL R&D program is presently underway at RRCAT. The aim of the first two stages of the program is to develop expertise in FEL design, development of FEL sub-systems, and to develop some state-of-the-art technologies like photoinjectors and short bunch diagnostics and manipulation techniques, while simultaneously building an IR-FEL based user facility. The third stage will build on the expertise developed in the first two stages to ultimately build a high power, short pulsed UV/VUV FEL with state-of-the-art electron beam quality and pulse structure that could also have potential applications for an X-ray FEL. Prior to the three-stage program, significant expertise was developed at RRCAT on FEL physics design issues through analytical studies and computer simulations.

CUTE-FEL development: The first stage of the FEL program at RRCAT formally began in 2002 with a project aimed at the development of a far infra-red FEL, called as the Compact Ultrafast Terahertz FEL (CUTE-FEL).This project was mooted as a technology demonstrator project and it envisaged the in-house development of all important sub-systems of the FEL like the linac and other accelerating structures, the electron beam transport line, the undulator, the klystron pulse modulator, etc. For the first time in the centre, an S-band linac structure was developed, characterized and used to accelerate a 90 keV electron beam from a thermionic electron gun to ~ 7 MeV in a 42 cm long structure. The linac structure developed for the project was a Plane Wave Transformer (PWT) type standing wave structure, which was the second operating linac of its type anywhere in the world. A 2.5 m long pure permanent magnet undulator was built in-house in two segments of 1.25 m each, and the magnetic field of the undulator was mapped using a measurement bench developed in-house to confirm compliance to design specifications.

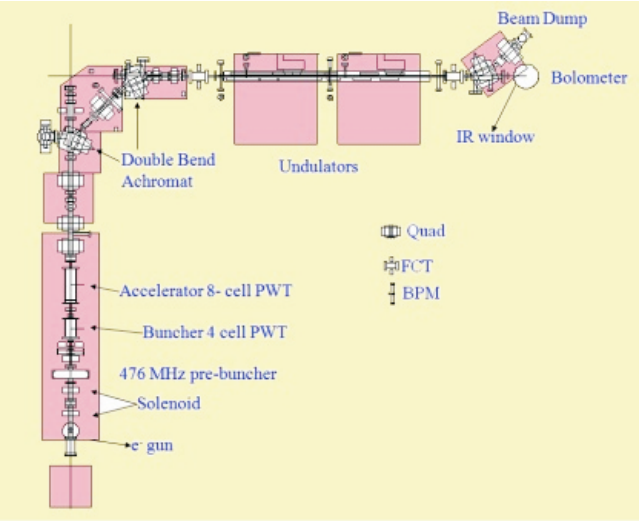


***Fig.T.2.3:*** *Schematic of the CUTE-FEL setup.*

Figure T.2.3 shows a schematic of the CUTE-FEL setup, and Table 1 summarizes the design electron beam and THz radiation parameters for the CUTE-FEL. The first signature of build-up of coherence in the CUTE-FEL setup was observed in 2012 [2], and further progress was not possible due to the non-availability of an important sub-system for powering the 476 MHz pre-buncher RF cavity and to generate the stable low level RF (LLRF) required for synchronous operation of three components, viz. electron gun at 36.615 MHz, sub-harmonic pre-buncher at 476 MHz and S-band linac at 2856 MHz.

*Table T.2.1: Design parameters of the CUTE-FEL and its sub-systems*

| Parameter | Value |
|---|---|
| Operating wavelength | 80-150 μm |
| Configuration | Oscillator |
| Out-coupled power | 0.4 MW (peak)/ 6 mW (CW average) |
| FEL radiation pulse width | 10 ps (FWHM) |
| **Undulator parameters** | |
| Type | Planar, NdFeB pure permanent magnet based |
| Period length ($\lambda_u$) | 50 mm |
| K parameter (peak) | 0.8 at 35 mm gap |
| No. of periods ($N_u$) | 50 |
| **Linac Parameters** | |
| Operating mode | π mode |
| Resonant frequency | 2856 MHz |
| Energy gain | 7-10 MeV |
| RF power | 3-7 MW |
| Type | SW, PWT |

*IR-FEL development:* The second stage of the FEL program at RRCAT is presently underway. In this stage, an infra-red FEL (IR-FEL) that is tunable in the wavelength range of 12.5 – 50 μm is being built to serve a user facility, where initial experiments have been planned in the area of Materials Research. Learning from the experience gained during the CUTE-FEL development, emphasis in the second stage was placed on in-house development of crucial low and high power RF systems for powering the RF cavities used in the injector linac system. This FEL is presently in an advanced stage of commissioning, and first lasing has recently been observed in the setup in November 2016. Further experiments are presently underway to optimize operation parameters to achieve saturation of the FEL.

Table T.2.2 summarizes the important specifications of the IR-FEL and its sub-systems. The physics design simulations of the IR-FEL dictate a requirement of 10 ps long electron bunches with 30 A peak current, normalized emittance $\leq$ 30 mm mrad, relative energy spread $\leq$ 0.5% and mean energy jitter < 0.4%. As per the design simulations, it takes ~ 80 round-trips for the FEL to reach saturation considering the above electron beam parameters and and the undulator parameters given in Table T.2.2. Details of the IR-FEL design simulations are given in [3]. In order to achieve

the desired electron beam parameters, injector design simulations have been performed to compare the two possible options – (1) using imported electron linac components viz. travelling wave buncher and SLAC type linac structure with an S-band pre-buncher in addition to a sub-harmonic pre-buncher structure developed in-house, and (2) sub-harmonic pre-buncher followed by two cascaded 12-cell PWT linac structures developed in-house. Both the design configurations have been optimized to achieve desired electron beam parameters at the exit of the injector system. Details of the injector design are given in [4].

*Table T.2.2: Design parameters of the IR-FELand its sub-systems*

| Parameter | Value |
|---|---|
| Operating wavelength | 12.5-50 μm |
| Configuration | Oscillator |
| Out-coupled power | 2 MW (peak)/ 15-30mW (CW average) |
| FEL radiation pulse width | 10 ps (FWHM) |
| Macro pulse width/ repetition rate | 10 μs / 1 - 10 Hz |
| **Undulator parameters** | |
| Type | Planar, NdFeB pure permanent magnet based |
| Period length ($\lambda_u$) | 50 mm |
| K parameter (RMS) | 1.2at 27 mm gap |
| No. of periods ($N_u$) | 50 |
| Error in peak field (RMS) | < 0.5% |
| Error in period (RMS) | < 0.05 mm |
| **Linac Parameters** | |
| Operating mode | 2π/3 mode |
| Resonant frequency | 2856 MHz |
| Energy gain | 15 - 25 MeV |

Initial commissioning has been performed with two cascaded 12-cell PWT linac structures developed in-house[5], which have delivered an energy gain of ~ 18.5 MeV consuming a total of ~ 6 – 7 MW during experiments on the IR-FEL setup. The total length of the two PWT linac structures is 126 cm, which translates to an accelerating gradient of ~ 19 MV/m for these structures. A train of 1 ns long electron bunches with 1 nC charge repeating at a frequency of 29.75 MHz for a macro-pulse duration of 10 μs is generated by a fast-pulsed thermionic electron gun. This is transported through a low energy electron beam transport line to a sub-harmonic pre-buncher RF cavity for bunching to ~ 50 ps before it is injected into the first 12-cell PWT linac structure for further bunching and acceleration to rated energy in the two PWT linac structures. The sub-harmonic pre-buncher structure employed in the IR-FEL injector system has also been developed in-house. Figure T.2.4 shows a picture of the IR-FEL injector linac system, starting with the high voltage deck of the electron gun on the right followed by a stainless steel pre-buncher and two 12-cell PWT linac structures on the left.

*Fig. T.2.4: IR-FEL injector linac section*

Since the IR-FEL operates in an oscillator configuration, there is an additional stringent requirement on the timing jitter between subsequent electron micro-bunches entering the undulator. A 10 ps long electron bunch propagating through the IR-FEL undulator generates a 10 ps long IR radiation pulse that co-propagates along the length of the undulator. As the electron and radiation pulse move down the undulator, there is a slippage in the electron bunch on account of the difference in velocities between the electron and optical pulses. This slippage is of the order of a couple of picoseconds, and it adversely affects the energy exchange between the electron bunch and the radiation pulse inside the undulator. To ensure sufficient overlap between the two, design simulations dictate that the jitter in arrival time of the electron bunches at the undulator entry should be $\leq 1 - 2$ ps. Beam dynamics simulations of the injector indicates that the timing jitter between micro-bunches of electrons in each macro-pulse depends critically on the phase of the RF fed to the pre-buncher as well as to the two PWT linac structures. Similarly, the jitter in mean energy of the electron micro-bunches depends critically upon the amplitude stability of the RF fed to these structures. Consequently, injector design simulations dictate a requirement of an RF flat-top < 0.4% over a macro-pulse duration of 10 μs with a phase stability of

1 degree at 2856 MHz over each macro-pulse. For the sub-harmonic pre-buncher, the requirement of phase stability is even more stringent.

The low and high power RF systems required to meet these stringent requirements for the IR-FEL setup have been developed in-house by the concerned expert groups in the Pulse High Power Microwave Division and the Radio Frequency Systems Division at RRCAT. Initial experiments on the IR-FEL setup indicate that some major design parameters for these systems have been achieved, while efforts are presently underway on fine-tuning system parameters to meet all the stringent operating parameters for the IR-FEL RF systems. Details of these RF systems developed for the IR-FEL can be found in [6,7].

The accelerated electron beam from the IR-FEL injector system is transported to the undulator entry through an electron beam transport line that has been designed to transport and manipulate a round beam at the linac exit to a flat beam with RMS beam sizes of 0.5 mm vertical x 1.5 mm horizontal at the undulator entry[8]. The transport line section has provision for electron beam diagnostics to measure size and position of the electron bunches, and the charge carried by each bunch. It also has provision for energy selection of the charge fraction having the desired relative energy spread in each accelerated electron bunch. The energy selection has been accomplished using a slit built in-house with independently movable arms for intercepting the low and high energy fractions of the accelerated bunch after a dispersive section of the transport line. Figure T.2.5 shows a picture of the IR-FEL electron beam transport line and its vacuum beamline [9].

***Fig. T.2.5:*** *IR-FEL electron beam transport line*

The accelerated electron beam transported during commissioning experiments has been characterized using the beam diagnostic systems provided in the IR-FEL electron beam transport line. Measurement of a typical electron beam spot at the undulator entry shows an RMS beam size of 1.25 mm vertical x 2.4 mm horizontal. The emittance $\varepsilon_x$ of the electron beam, measured using a quadrupole scan method, is ~45 mm mrad, which is within acceptable limits.

The IR-FEL setup employs a 2.5 m long, pure permanent magnet undulator that has been procured from M/s Kyma srl, Italy. Before installation as part of the IR-FEL setup, it has been subjected to detailed field mapping at the supplier's site as well as at RRCAT to ensure field quality is as specified by the physics design of the IR-FEL. It is installed inside the 5.04 m long optical cavity of the IR-FEL, which has two gold-coated copper mirrors with slightly different radii of curvature in a near concentric configuration [3]. The downstream mirror has a 3 mm hole for out-coupling of a fraction of the intra-cavity IR power. The spent electron bunches are bent out of the optical cavity and transported to a suitably designed beam dump with sufficient supplementary shielding to ensure radiation levels in normal occupancy areas outside the shielded area are within permissible limits. Figure T.2.6 shows a picture of the IR-FEL undulator with its vacuum beam pipe, which has a race-track inside cross-section. The downstream mirror is mounted on a precision six-axis hexapod for scanning the cavity length during experiments on lasing. The up-stream mirror is presently supported on a rigid frame, and has been locked in place after alignment.

*Fig. T.2.6: IR-FEL undulator & its vacuum chamber beam transport line*

*Commissioning of the IR-FEL:* After an initial period of RF conditioning of the linac structures with progressively increasing pulse width and power levels, beam transmission experiments were performed to optimize transmission of an accelerated electron beam through the undulator. The first electron beam transport through the undulator was achieved in January 2016, which resulted in the first measurement of IR power generated in the setup. The IR radiation generated was measured using a liquid helium cooled bolometer (QMC, QGeB2). Further optimization of electron beam transport through the setup resulted in the generation of copious amounts of IR radiation leading to saturation of the bolometer. These initial experiments were performed without the downstream mirror to out-couple all the IR radiation generated by the setup.

After installation of the downstream mirror and alignment of the optical cavity, experiments were performed to study lasing in the IR-FEL setup. The measured electron beam parameters in these experiments were: electron beam energy - 18.4 MeV, charge per pulse – 0.26 nC, and normalized RMS emittance – 45 mm mrad. The experiments were performed with the beam slit set to select charge with a relative energy spread ~ 0.75 %. Figure T.2.7 shows the ICT traces at different locations along the beam transport line, with ICT5 corresponding to the ICT at the undulator exit.


*Fig. T.2.7:ICT traces at different locations in the IR-FEL setup*

With the installation of the down-stream mirror, only ~ 5% of the intra-cavity power is out-coupled through the 3 mm hole in the mirror. The position of the downstream mirror was varied using the hexapod, initially in steps of 8 μm and subsequently in steps of 2 μm. A sudden steep increase in the out-coupled power was measured when the length of the optical cavity approached the design length of 5038.528 mm. At this cavity length, the bolometer showed a very high degree of saturation. Figure T.2.8 shows the saturated bolometer trace for the experiments. The measured enhancement of ~ $10^5$ times over expected spontaneous radiation power for the electron beam parameters used in the experiment is the first observation of lasing in the IR-FEL setup. It is also the first reported lasing of an FEL in the country. Experiments are presently underway on optimizing electron beam and RF parameters to achieve saturation in the IR-FEL. This will lead to a further enhancement in gain by ~ two orders of magnitude.

*Fig. T.2.8: Saturated bolometer signal during lasing*

## 6. Status of FEL R&D worldwide

FELs now have a proven track record as indispensable tools for scientific research at wavelengths ranging from the mid infra-red to THz/mm waves, and at X-ray wavelength. Many user facilities like the FELIX facility in Netherlands, the CLIO facility in France, the IFEL in Japan, etc. are being used as user facilities for cutting-edge research in different areas of science and technology. The FEL facility at the IFELin Japan has demonstrated ability to operate at wavelengths ranging from 0.23 mm to 100 mm using five different undulators[10]. THz/IR FELs have also been built for strategic applications to deliver from few kW of CW average power at Novosibirsk [11] to few tens of kW of CW average power at the Thomas Jefferson lab [12]. Different configurations of THz FELs have been explored with emphasis on compact sources using short linac and undulator sections [13].

FEL facilities designed to operate in the hard/soft X-ray region are usually built around existing or planned accelerator facilities producing high quality GeV beams, viz. LCLS at

SLAC, SACLA at Spring 8, FLASH at BESSY. FELs in the far infra-red (far IR) and Terahertz (THz) region on the other hand require modest electron beam energies with relatively shorter undulator sections, and are more widespread in universities and research institutes. Internationally, two hard X-ray FELs are presently in operation at the LCLS in the USA and at SACLA in Japan. At least three more hard X-ray FELs are expected to lase shortly, viz. the European XFEL in Germany, the Swiss XFEL at the Paul Scherer Institute in Switzerland and at the Pohang Light Source in Korea. Many other laboratories like the FERMI and SPARX FELs in Italy have built soft X-ray FELs employing alternate seeding schemes like harmonic generation, high gain harmonic generation, etc. Reference [14] presents an illuminating review of the present worldwide status of FEL development at hard X-ray as well as soft X-ray wavelengths. The worldwide status of FEL development is summarized in the form of tables in Reference [15].

**Conclusion:**

FELs area now accepted as indispensable tools for cutting-edge research in different areas of science and technology. The principle of operation of an FEL, different configurations of FELs and the advantages offered by FELs over conventional lasers have been discussed in this article. The R&D activity on FELs at RRCAT, and the status of FEL R&D worldwide has been briefly discussed in this article.

**References:**


[1] C.A. Brau, Free Electron Lasers (Academic, San Diego, 1990); Vinit Kumar, Some Studies on Free Electron Laser Oscillators, Ph.D. Thesis, 2003; T.C. Marshall, Free Electron Lasers (Macmillan, New York, 1985); K.K. Pant, Free Electron Lasers(Ed. P.K. Gupta and Rajeev Khare, World Scientific, Singapore, 2014).

[2] B. Biswas et al., Current Science, vol.105(1), 26, 2013.

[3] Vinit Kumar et al., Proc. InPAC 2011, IUAC, New Delhi (2011).

[4] Arvind Kumar et al., Proc. InPAC 2009, RRCAT, Indore, (2009).

[5] Saket Gupta et al., Proc. InPAC 2015, TIFR, Mumbai (2015).

[6] P. Shrivastava, RRCAT Newsletter, 29(1), 2016; P. Mohania et al., Proc. InPAC 2015, TIFR, Mumbai (2015)

[7] Gautam Kumar et al., Proc. InPAC 2015, TIFR Mumbai (2015); Nitesh Tiwari et al, Proc. InPAC 2015, TIFR, Mumbai (2015).

[8] R.S. Saini et al., Proc. InPAC 2011, IUAC, N. Delhi (2011), Kailash Ruwali et al, Proc. InPAC 2015, TIFR, Mumbai (2015); Alok Singh et al, Proc. InPAC 2015, TIFR, Mumbai (2015).

[9] V. Sathe et al, Proc. InPAC 2015, TIFR, Mumbai (2015).

[10] H. Horike et al., Proc. FEL Conf., p. 251 (2004).

[11] G. Kulipanov et al., IEEE Trans. THz Sci. Tech., 5(5), 798 (2015).

[12] S. Benson et al., Proc. IEEE PAC, p.79 (2007).

[13] G.P. Gallerano et al., J. Infrared, Millimeter and THz Waves, 35, 13 (2014).

[14] C. Pellegrini et al., Rev. Mod. Phys., 88, 015006-1 (2016).

[15] K. Cohn et al, Proc. FEL Conf, p. 625, Korea (2015).